

BACHELOR

Electron temperatures in an Argon plasma

Penterman, K.E.M.

Award date:
2012

[Link to publication](#)

Disclaimer

This document contains a student thesis (bachelor's or master's), as authored by a student at Eindhoven University of Technology. Student theses are made available in the TU/e repository upon obtaining the required degree. The grade received is not published on the document as presented in the repository. The required complexity or quality of research of student theses may vary by program, and the required minimum study period may vary in duration.

General rights

Copyright and moral rights for the publications made accessible in the public portal are retained by the authors and/or other copyright owners and it is a condition of accessing publications that users recognise and abide by the legal requirements associated with these rights.

- Users may download and print one copy of any publication from the public portal for the purpose of private study or research.
- You may not further distribute the material or use it for any profit-making activity or commercial gain

Eindhoven University of Technology
Department of Applied Physics
Elementary Processes in Gas discharges

Electron temperatures
in an Argon plasma
Kathelijne Penterman

August 2012

EPG-12-16

Under Supervision of:
Dipl. Phys. S Hübner
Prof Dr. J J A M v d Mullen

Summary

For this report a microwave induced plasma has been studied. This plasma was created using a surfatron design. The light emission of the plasma was measured and calibrated to find the absolute intensity of the light. With the absolute intensity the absolute excited state densities could be calculated. By comparing these densities to calculated densities from a CR model, with given electron temperature and electron density, the electron temperature, T_e , can be measured. This is called the ALI method [1].

That has been done in an Argon plasma under several conditions. To calculate T_e the spectrum of the emitted light has been measured at several wavelengths. Which wavelength is used to calculate T_e matters for the result, however. When the intensity measured at 763,5 nm (2p6 state) was used, the result showed a distinct offset from the results measured with the intensities at the other wavelengths. Yet, each result show similar dependencies under changing plasma conditions.

Firstly the pressure was varied. These measurements show that T_e decreases as the pressure rises.

Secondly the spatial position was varied. The plasma has been created in a tube and T_e was measured from the beginning to the end of the plasma. These measurements show that T_e is constant along the tube, except at the very end, where it drops suddenly.

The results at lower pressures agree nicely with those from earlier measurements. However the results of the measurement axially along the plasma column showed a different result compared to some earlier measurements with Thomson scattering [1], in which the temperature rises at the end of the plasma, instead of drops. A possible reason for that difference lies in the different methods. Thomson scattering gives the mean energy of the plasma, while $T_e(\text{ALI})$ is a temperature associated with the excitation flux.

Despite that difference the results are found reliable, since the drop at the end has been observed before, when using the ALI technique. These results may partially also be caused by a change in the radial shape at the end of the plasma.

Lastly, the error in T_e was usually roughly around 10 to 20 %. This causes the results to be somewhat uncertain, but still results at lower pressures and along the tube show significant decays.

Contents

Summary	1
Contents	2
Introduction.....	3
1 Theory	4
1.1 Plasmas	4
1.2 Absolute intensity measurements	4
1.3 Line radiation	4
1.4 ASDF	4
1.5 Electron temperature.....	5
2 Experimental setup.....	6
2.1 Plasma setup.....	6
2.2 Optical setup	6
2.3 Calibration.....	6
2.4 Electron temperature.....	7
2.5 Error Analysis	7
3 Results and discussion	9
3.1 ASDF	9
3.2 Higher pressures.....	9
3.3 Lower pressures	10
3.4 Measuring along the tube.....	11
3.5 Discussion	11
4 Conclusion	13
5 References.....	14
Appendix A.....	15
Appendix B	16

Introduction

It is roughly estimated that about 99.9% of the known matter of the universe consists of plasma, which may not be so surprising since all stars consist of plasma. But also back on earth plasmas play a role. Lightning is a good example of naturally occurring plasmas. So understanding how a plasma works exactly, seems to be vital for the understanding of our universe. Sadly however, plasmas are not nearly as well understood as other states of matter, simply because there has been far less research into plasmas as into, for example, solids. They were only first identified in the late 1800's and are rather difficult to study, since they are gaseous and consequently low in density and volatile.

However, plasmas are being used in some of the newest technology. It is for example used for atomic layer deposition, a method that uses a plasma to create a layer of one atom thick upon a surface. There has also been extensive research into the application of plasmas in medicine lately. It appears to be very useful, both in disinfection and in wound healing.

So not only for scientific, but also for practical purposes, it is useful to understand the nature and workings of plasmas. And to increase our understanding it is vital to perform measurements.

Luckily, plasmas glow, which may turn out to be one of their best assets. Because of this we can measure the light a plasma emits and use this to try and understand its inner workings. That is what has been done for this report. The emission of a plasma, in this case created from Argon using microwaves, is measured and from this emission the electron temperature T_e in the plasma is calculated, using a model to map the plasma's expected behaviour. T_e is a key parameter to understand the excitation kinetics of a plasma.

In time, with enough scientists working on plasmas, doing different measurements and checking and cross-checking each other's work, a full image of the workings of plasmas in several conditions may be found and armed with this, man will be able to apply them to their fullest extent.

1 Theory [1]

1.1 Plasmas

Plasmas are usually viewed as the fourth state of matter. Unlike the other three states, however, the atoms do not retain their form in a plasma. A plasma is a mixture of atoms, ions and free electrons. One of the ways to create a plasma, is by using microwaves. The energy of the microwaves frees some electrons, thus creating a mixture of plasma and gas, which behaves like a plasma.

One of the nice things about plasmas is that they emit light. This of course makes them shiny, but it is also great for plasma research. Analyzing the light the plasma naturally emits is called passive spectroscopy, contrary to active spectroscopy, in which case a laser is pointed at the plasma.

1.2 Absolute intensity measurements

Apart from relative spectroscopy or other active research methods, it is also possible to look at absolute light emission values from the plasma. The relative method is often preferred, since no calibration needs to be done and this makes it much easier. However to deduce state distributions and temperatures from that is difficult. This typically needs the establishment of a Saha-Boltzmann distribution. But when there are large deviations from Saha-Boltzmann, as is the case with large effluxes of electron-ion pairs from the plasma, the relative method doesn't work well or needs very extended models. Therefore absolute intensity measurements are performed instead, even though these do require calibration. This allows to determine the excited state densities and compare these to the ground state. This comparison yields more crucial information about the distribution.

1.3 Line radiation

The photons emitted by a plasma originate from several sources. One of them is the excitation of electrons in an atom or ion. When these electrons fall back to a lower energy level a photon with a specific frequency is emitted. By studying the intensity of light at several wavelengths, a lot can be learned about the plasma, because the intensities depend on, among others, the electron density and the electron temperature.

1.4 ASDF

To analyze the plasma an atomic state distribution function (ASDF) can be made. The ASDF shows the amount of atoms per state on a logarithmic scale at each energy level. In order to calculate this, the absolute intensity at certain wavelengths is measured and the following formula is used (see Appendix B):

$$n(u) = \frac{4\pi(I_{ul}/D)}{A(u,l)E_{lu}} \quad (1),$$

in which $n(u)$ is the amount of atoms at level u , I_{ul} is the intensity of light corresponding to the energy E_{lu} between level u and l , the level below u , D is the magnitude of the measured surface and $A(u,l)$ is the probability an electron will go from u to l .

However, instead of the amount of atoms on a level $n(u)$, the amount of atoms per statistical weight on a level $\eta(u)$ is needed for the ASDF:

$$\eta(u) = n(u)/p(u) \quad (2),$$

in which $p(u)$ is the amount of states at level u .

The ASDF is now made by plotting the natural logarithm of $\eta(u)$ against the corresponding energies E_{iu} .

1.5 Electron temperature

From the ASDF it is possible to calculate the electron temperature T_e . The slope in the ASDF corresponds to a certain temperature. However the electron temperature can only be calculated this way if Saha-Boltzmann (SB) is followed. Since this is not the case, the deviation from SB, $r^1(p)$, needs to be calculated.

A model [3] is used to calculate $r^1(p)$. This model mimics the workings of the plasma, but to get $r^1(p)$, T_e is set first. And to calculate T_e , $r^1(p)$ is necessary. Thus, a comparison is needed. $r^1(p)$ is calculated for many T_e -values. The experimental values are compared with a starting $r^1(p)$ giving a starting T_e . This new T_e is used in the model for another r^1 . That can be iterated until convergence is reached.

To calculate T_e the following formula is used (see Appendix B):

$$T_e = \frac{1}{k_B} \frac{E_{1p}}{\ln(r^1(p)\eta(1)/\eta(p))} \quad (3),$$

in which k_B is Boltzmann's constant and E_{1p} is the energy difference between level p and ground state.

When looking at Argon, usually the 4p group ($p = 3$) is used for calculations, since this is the lowest level, that can be easily detected. It is also the most easily visible.

The value of $\eta(1)$ is given by the pressure, using the following formula:

$$\eta(1) = \frac{p}{k_B T_g} \quad (4).$$

2 Experimental setup [1]

2.1 Plasma setup

To create the plasma, a surfatron is used (Figure 1). A microwave generator is connected to this surfatron, to ignite an Argon gas, flowing through a hollow tube with variable pressure. The tube is placed through the launching gap. The plasma extends from this launcher along the tube, because a surface wave builds up. Typical lengths of 10 to 30 cm are reached.

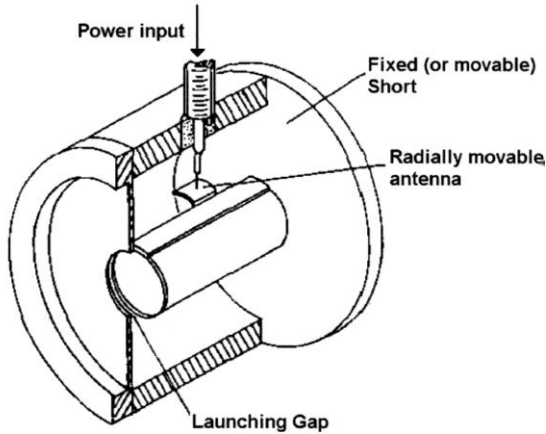


Figure 1: A cross-section of the surfatron. Components have been named. [2]

2.2 Optical setup

Perpendicular to the plasma tube, a lens is placed. This lens collects the light, emitted by the plasma. Because the light first passes through a gap in front of the lens, the observation volume is smaller than the actual plasma diameter. The lens is connected by an optical fiber to a spectrometer, which converts the light into a spectrum and shows the intensity of the light at several wavelengths.

2.3 Calibration

Absolute intensity measurements require calibration. For calibration a tungsten ribbon lamp with a known light spectrum is used. Using the same method as is used to measure the intensity of the light emitted by the plasma, the known intensity of the lamp is measured. It is not necessary to measure the entire spectrum, a select group of wavelengths, the same as used to create the ASDF, will do. It is important however to take the size of the plasma and the size of the lamp into account, because the greater the surface of the emitter, the higher the intensity of the measured light will be. The measured intensities of the lamp are then compared to their known values. Using both all future measurements can also be calibrated easily:

$$I_r = RI_m \frac{I_k}{I_c} \quad (5),$$

in which I_r is the real intensity of the plasma, I_m is the measured intensity of the plasma, I_k is the known intensity of the tungsten ribbon, I_c is the measured intensity of the tungsten ribbon at a certain wavelength and R is the ratio of the measured surface

of the lamp divided by the measured surface of the plasma. The experimental value of $R = 0,77 \pm 0,5$.

2.4 Electron temperature

First the electron temperature is measured at different pressures. It is measured close to the launching gap, as seen in Figure 1. The assumption here is that the emittance is constant along the plasma, at least at the first half of the column.

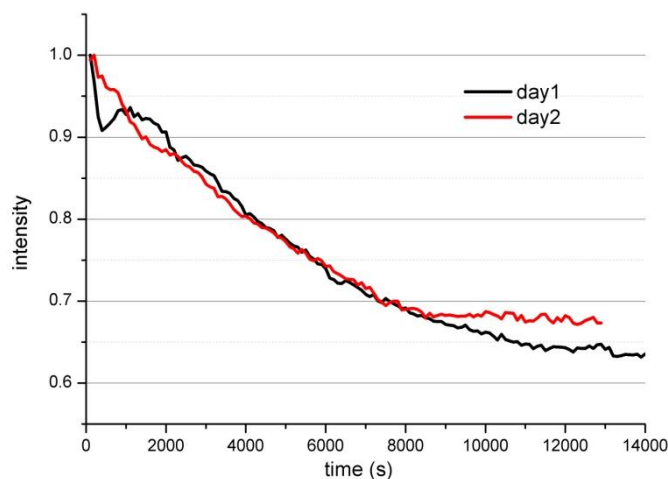
To verify this assumption and get an image of T_e along the whole tube, it was also measured at several places along the tube. The distances are measured from the launching gap, as seen in Figure 1.

2.5 Error analysis

In this case the error-margin of T_e consists of a systematic and random error. A known systematic error will be accounted for and the unknown errors will be estimated and taken into account in the discussion of the results.

The systematic error was only spotted first after several measurements had already been done, being the measurements at pressures ranging from about 20 to 80 mbar. It is therefore impossible to check whether or not the phenomenon occurred during these measurements and it cannot be accounted for. However these measurements were done over a time of two days and the ratio of intensities R , given by dividing the intensities at the start of the second day by the intensities of at the start of the first day and averaging this, gives a value of $R = (1,24 \pm 0,07)$. This can be used to at least plot these results together.

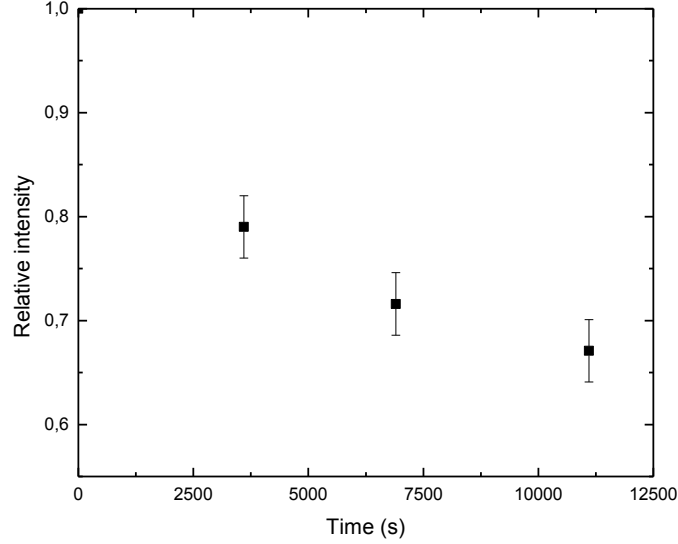
Mapping the decay of the response of the spectroscopical system at two later days, gave the following graph:



Graph 1: The relative intensity as a function of time from the moment of starting up the measuring equipment.

During the other measurements, checks were performed to be able to calculate the relative intensity and match it (see Graph 2).

As Graphs 1 and 2 show, the decay during measurements matches the mapped decay, which can therefore be used to shift the measured intensities to their proper positions.



Graph 2: The measured relative intensity as a function of time from the moment of starting up the measuring equipment.

The random error in T_e , ΔT_e , can be calculated with the following formula:

$$\Delta T_e(p) = \left| \frac{\partial T_e}{\partial r^1(p)} \right| \Delta r^1(p) + \left| \frac{\partial T_e}{\partial \eta(1)} \right| \Delta \eta(1) + \left| \frac{\partial T_e}{\partial \eta(p)} \right| \Delta \eta(p) \quad (6)$$

$$\rightarrow \Delta T_e(p) = \frac{T_e}{\ln(r^1(p)\eta(1)/\eta(p))} \left(\frac{\Delta r^1(p)}{r^1(p)} + \frac{\Delta \eta(1)}{\eta(1)} + \frac{\Delta \eta(p)}{\eta(p)} \right) \quad (7),$$

in which (see Formula 1 and 2):

$$\frac{\Delta \eta(p)}{\eta(p)} = \frac{\Delta n}{n} = \frac{\Delta I_{u,l}}{I_{u,l}} + \frac{\Delta D}{D} \quad (8),$$

The offset of $\eta(1)$ is given by (see Formula 4):

$$\frac{\Delta \eta(1)}{\eta(1)} = \frac{\Delta p}{p} + \frac{\Delta T_g}{T_g} \quad (9),$$

in which T_g is the gas-temperature.

So ΔT_e equals:

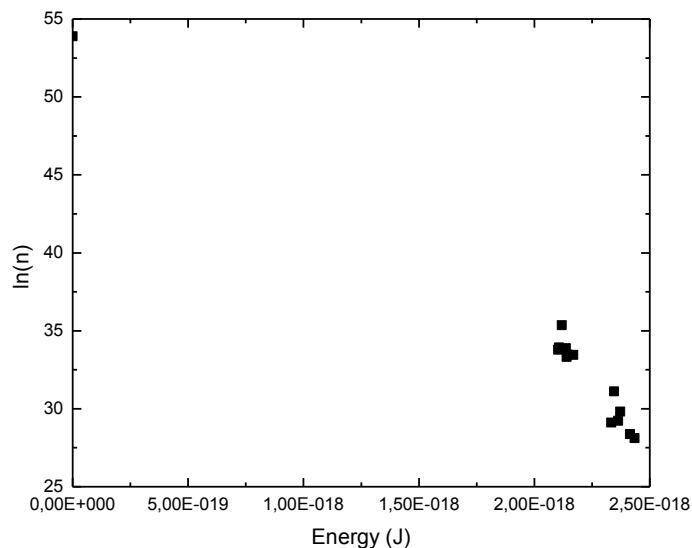
$$\Delta T_e(p) = \frac{T_e}{\ln(r^1(p)\eta(1)/\eta(p))} \left(\frac{\Delta r^1(p)}{r^1(p)} + \frac{\Delta p}{p} + \frac{\Delta T_g}{T_g} + \frac{\Delta I_{u,l}}{I_{u,l}} + \frac{\Delta D}{D} \right) \quad (10).$$

The random error in T_e ranges from about 10 to 20 %.

3 Results and discussion

3.1 ASDF

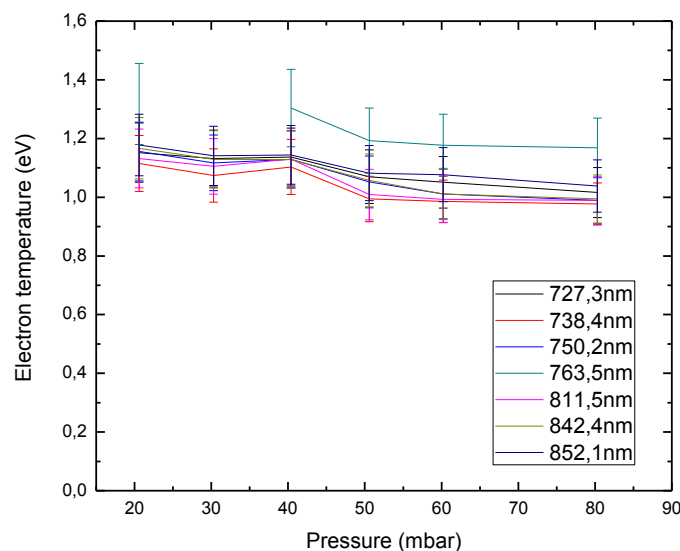
Graph 3 shows a typical example of an ASDF, as measured for this report. This one was calculated at a pressure of 11,4 mbar. The lens was placed at 2 cm from the launching gap of the surfatron.



Graph 3: The ASDF at 11,4 mbar, as measured at 2 cm from the launching gap of the surfatron. It shows the logarithm of the state densities at their respective energy levels.

The first group of data points, at approximately $2,2 \cdot 10^{-18}$, is the 4p-group. The slope between the first data point, the ground state, and the 4p-group, is used to calculate T_e .

3.2 Higher pressures



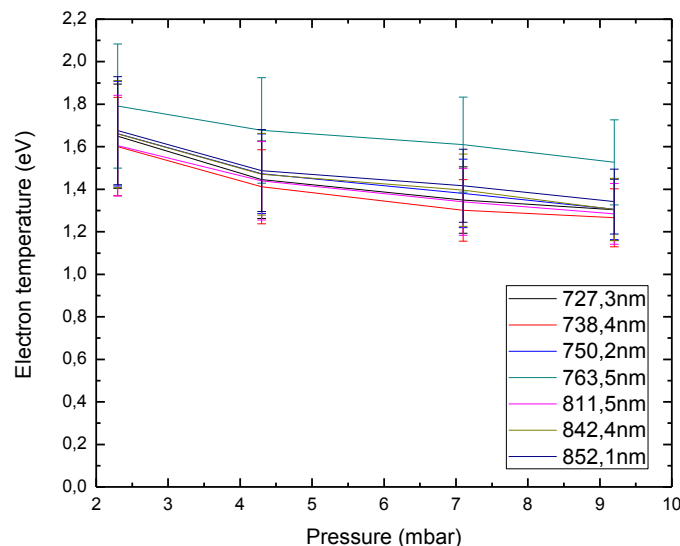
Graph 4: The electron temperature, calculated with different wavelengths, as a function of the pressure.

Applying the CR model to that ASDF determines the electron temperature. Graph 4 shows that for pressures from about 20 to 80 mbar, measured by using several wavelengths in the 4p-group.

As the graph shows, the electron temperature decreases at higher pressures, but not significantly as the error margin is usually about 10 to 20 % of the calculated temperature. Also the graph shows that when using different wavelengths, the electron temperature behaves roughly the same, only with a notable offset for the 4p-state which corresponds to the emission at 763,5 nm. This offset can also be seen in graph 3; it corresponds to the data point slightly above the rest of the 4p-group.

3.3 Lower pressures

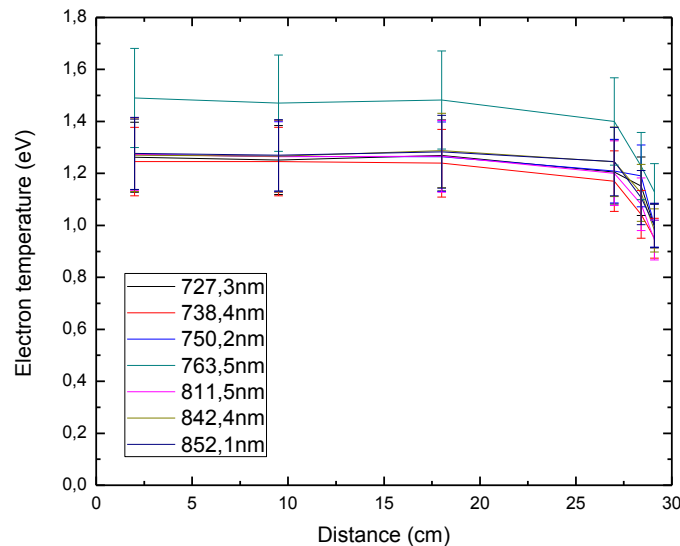
Graph 5 shows the electron temperature at pressures from about 2 to 10 mbar, measured by using several wavelengths in the 4p-group. It shows that the electron temperature decreases at higher pressures. It is also significantly higher than in graph 4, which shows T_e at higher pressures. The error-margin is somewhat greater, but when comparing the values at 2 mbar to those at 9, there seems to be a significant difference at some wavelengths. The different wavelengths still behave roughly the same, but with a still with a significant offset at 763,5 nm.



Graph 5: The electron temperature, calculated with different wavelengths, as a function of the pressure.

3.4 Measuring along the tube

Graph 6 shows the electron temperature at 11.4 mbar at different distances along the plasma. The same has been done at 2.3 and 79.6 mbar (Appendix C).



Graph 6: The electron temperature, calculated with different wavelengths, as a function of the distance from the launching gap of the surfatron, at 11,4 mbar and a plasma length of 22 cm.

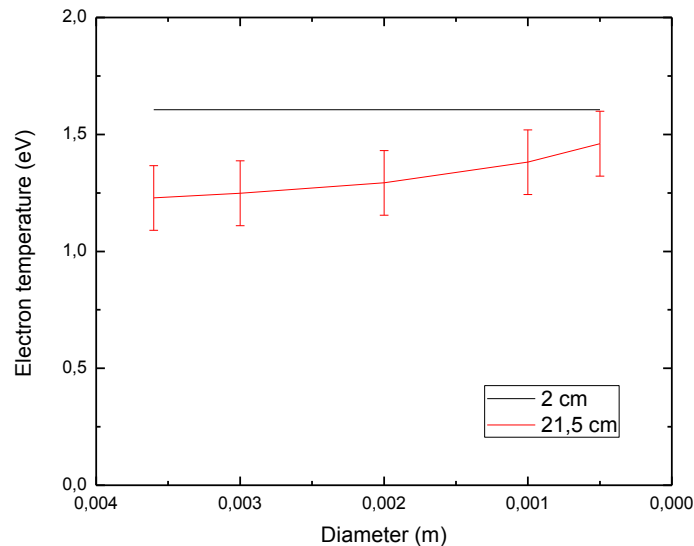
3.5 Discussion

The results at higher pressures are not very trustworthy, because the measuring apparatus showed a decrease over time later (see 2.5) and it is unknown whether this was already the case during these measurements. Correcting for the systematic error as if it were present, shows visible changes, but given the large random error the changes are not significant. Furthermore, the systematic decrease in electron temperature along the plasma column was expected, since it has been measured before, using both the method used here and other methods [1].

The results at lower pressures are quite trustworthy. As 2.5 shows, the systematic error, created by the measurement equipment, can be accounted for here. Also the decrease in electron temperature is as it is expected, compared to other measurements using both the method used here and other methods [1].

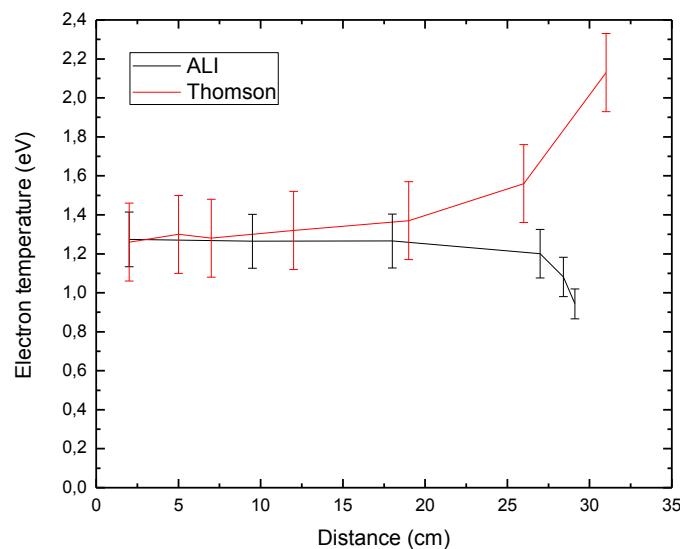
A possible cause for the observation of a lower T_e at the end of the plasma column, is that the plasma's shape might change. This could result in a lower diameter and thus a different T_e . If the diameter was different, this was not taken into account in the calculations. To see how big the effect is, if the wrong diameter was used for the calculations, T_e has been calculated with different assumed diameters. The result can be seen in graphs 7 ad 12 (also see Appendix C).

As can be seen in graphs 7 and 12 this could partially explain the lowering of the temperature at the end. The diameter of the plasma is 6 mm. The detection volume diameter is smaller however, since a tube with a small gap is placed in front of the lens, that collects the light. The graphs show that the actual diameter of the plasma and thus the diameter of the detection volume should have been about a sixth of the diameter of plasma at the start of the tube to completely explain the increase in electron temperature. Since this comparison was done for a measurement near, but not quite at, the end of the plasma, such a decrease is rather unlikely.



Graph 7: The electron temperature shown when a different observation diameter is assumed at 2,3 mbar and 811,5 nm and with a length of 22 cm. The black line is the temperature at the base of the plasma (with a known diameter of 3,6 mm) and thus the reference line. The red line is taken near, but not at, the end of the plasma.

Thomson measurements also show a different result at the end of the plasma (Graph 8) [1].



Graph 8: The electron temperature as a function of the distance from the end of the plasma, calculated by using both Thomson scattering [4] and the ALI method at 811,5 nm. The pressure is about 10 mbar and the plasma length is about 30 cm.

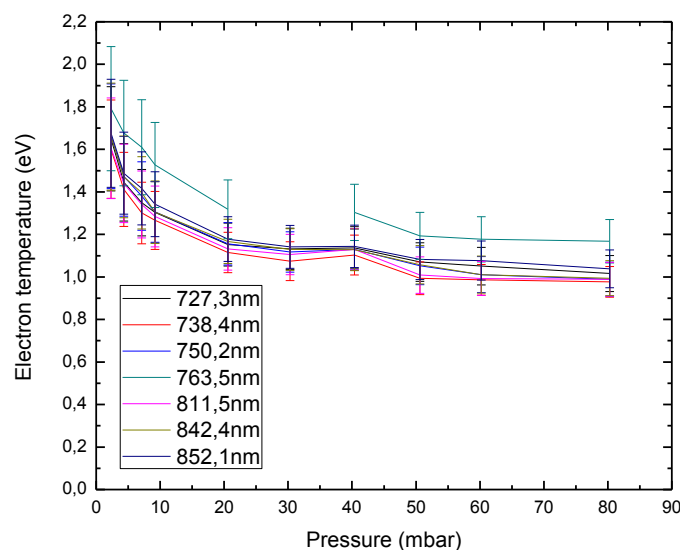
These measurements show a rise in temperature, instead of a drop. A possible reason for that difference lies in the different methods. Thomson scattering gives the mean energy of the plasma, while $T_e(\text{ALI})$ is a temperature of the excitation flux. That these two temperatures differ at the end of the plasma column might imply a change of the electron energy distribution function.

Lastly, given the used technique is correct, the result is quite also trustworthy. The systematical error has been accounted for. Furthermore, graphs 6, 10 and 11 all show this same result.

4 Conclusion

The technique used for this report is very easily applicable to gain a decent result for the electron temperature. The problems caused by the malfunctioning equipment, causing a systematic error, make it harder and less reliable, though.

What can be safely concluded from this report, is that the electron temperature in an Argon plasma, created by a surfatron, drops systematically as the pressure rises (Graph 9). That is because at lower pressure the losses by diffusion of electron-ion pairs to the wall are higher, thus the higher losses “demand” a higher T_e in order to sustain the plasma. As the diffusion scales with $1/n(1)$ the temperature drops for higher pressure.



Graph 9: The electron temperature, calculated with different wavelengths, as a function of the pressure.

This result is in agreement with earlier measurements, performed with different techniques and therefore quite reliable. The error-margins are quite big however, which makes the results, mainly at high pressures, somewhat less reliable. The error in $r^l(p)$ (see Formula 10) is the main contributor to the random error, with a relative error of 50 %. There is also a clear offset between the temperature calculated with the 763,5 nm spectrum and the other temperatures. The cause of this is unclear. The state measured at 763,5 nm does not seem to differ from the other states though, except that a higher intensity is measured at this wavelength.

The performed measurements also make it clear that the electron temperature drops at the end of the plasma-column. This is a significant result, not only seen in the three graphs in this report, but also in other measurements using this same method. It does contradict other sources. With the systematic error accounted for, these results are quite accurate. Even with the large error margin, the temperature is still lower at the end of the tube, than at the beginning. This phenomenon will need further study to understand, but it might be partially caused by the plasma changing shape near the end.

5 References

- [1] *Poly-diagnostic Validation of Spectroscopic Methods*, Ekaterina Iordanova, Eindhoven, Technische Universiteit Eindhoven (2010)
- [2] *Validation of diagnostics by use of polydiagnostics*, M.G. Ham, Eindhoven, Technische Universiteit Eindhoven (2008), p.4
- [3] *Zero-Dimensional models for plasma Chemistry*, Wouter Graef, Eindhoven, Technische Universiteit Eindhoven (2012)
- [4] *Thomson scattering on Argon surfatron plasmas at intermediate pressures: Axial profiles of the electron temperature and electron density*, J.M. Palomares, Eindhoven, Technische Universiteit Eindhoven (2010)

Appendix A

Wavelength (nm)	Lower Level			Upper Level		
	Configuration	Term	J	Configuration	Term	J
727,3	$3s^23p^5(^2P^{\circ}_{3/2})4s$	$2[{}^3/2]^{\circ}$	1	$3s^23p^5(^2P^{\circ}_{1/2})4p$	$2[{}^1/2]$	1
738,4	$3s^23p^5(^2P^{\circ}_{3/2})4s$	$2[{}^3/2]^{\circ}$	1	$3s^23p^5(^2P^{\circ}_{1/2})4p$	$2[{}^3/2]$	2
750,2	$3s^23p^5(^2P^{\circ}_{1/2})4s$	$2[{}^1/2]^{\circ}$	1	$3s^23p^5(^2P^{\circ}_{1/2})4p$	$2[{}^1/2]$	0
763,5	$3s^23p^5(^2P^{\circ}_{3/2})4s$	$2[{}^3/2]^{\circ}$	2	$3s^23p^5(^2P^{\circ}_{3/2})4p$	$2[{}^3/2]$	2
811,5	$3s^23p^5(^2P^{\circ}_{3/2})4s$	$2[{}^3/2]^{\circ}$	2	$3s^23p^5(^2P^{\circ}_{3/2})4p$	$2[{}^5/2]$	3
842,4	$3s^23p^5(^2P^{\circ}_{3/2})4s$	$2[{}^3/2]^{\circ}$	1	$3s^23p^5(^2P^{\circ}_{3/2})4p$	$2[{}^5/2]$	2
852,1	$3s^23p^5(^2P^{\circ}_{1/2})4s$	$2[{}^1/2]^{\circ}$	1	$3s^23p^5(^2P^{\circ}_{1/2})4p$	$2[{}^3/2]$	1

Appendix B

The derivations of the formulas in this report can be found below.

When an atom decays, a photon is emitted. The corresponding emission coefficient $j_{ul}(\lambda)$ equals:

$$j_{ul}(\lambda) = \frac{A(u,l)E_{lu}n(u)\varphi_\lambda(\lambda)}{4\pi} \quad (11),$$

in which $\varphi_\lambda(\lambda)$ is normalized in such a way that:

$$\int_T \varphi_\lambda(\lambda)d\lambda = 1 \quad (12),$$

in which T refers to the fact that the integral is carried out over the complete spectral line.

In the plasma used for this report:

$$I_\lambda(\lambda, D) = j_\lambda(\lambda)D \quad (13).$$

From Formula 11, 12 and 13 follows Formula 1:

$$n(u) = \frac{4\pi(I_{ul}/D)}{A(u,l)E_{lu}} \quad (1).$$

At a certain point p in the ASDF the population density $\eta(p)$ can be described as an addition of two contributions:

$$\eta(p) = \eta^1(p) + \eta^+(p) \quad (14).$$

These contributions can be related to the Boltzmann and Saha population densities, respectively $\eta^B(p)$ and $\eta^S(p)$, as follows:

$$\eta^1(p) = r^1(p)\eta^B(p) \quad (15)$$

and

$$\eta^+(p) = r^+(p)\eta^S(p) \quad (16).$$

In the case of strongly ionized plasmas this reduces to:

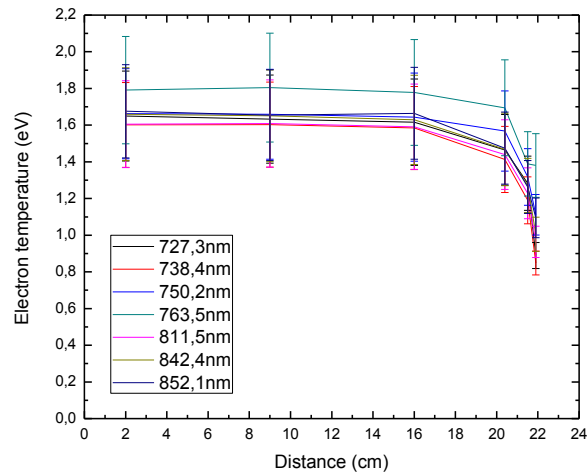
$$\eta(p) = r^1(p)\eta^B(p) = r^1(p)\eta(1)e^{-E_{1p}/k_B T_e} \quad (17)$$

$$\rightarrow k_B T_e = \frac{E_{1p}}{\ln(r^1(p)\eta(1)/\eta(p))} \quad (18)$$

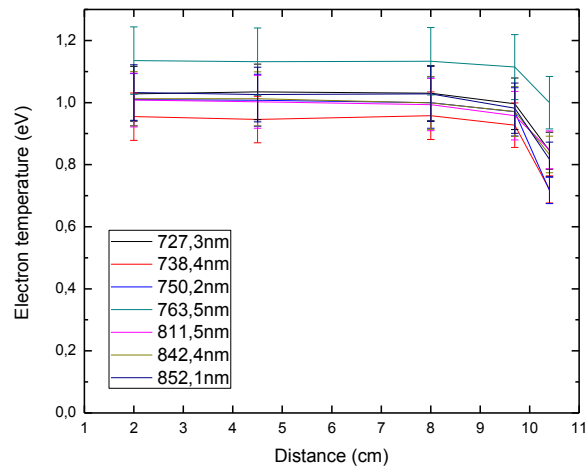
$$\rightarrow T_e = \frac{1}{k_B} \frac{E_{1p}}{\ln(r^1(p)\eta(1)/\eta(p))} \quad (3),$$

which is Formula 3.

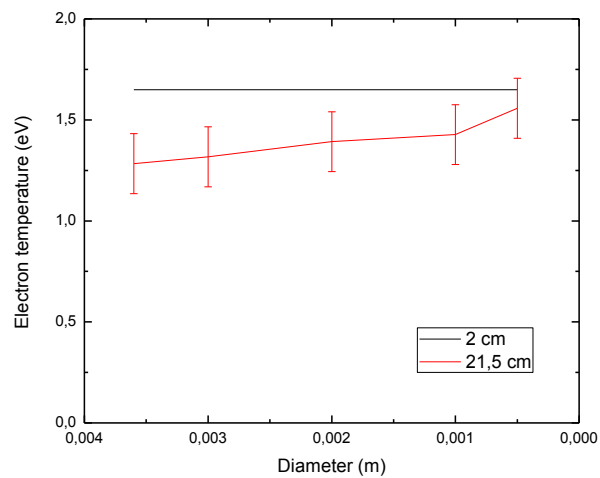
Appendix C



Graph 10: The electron temperature, calculated with different wavelengths, as a function of the distance from the launching gap of the surfatron, at 2,3 mbar and a plasma length of 29 cm.



Graph 11: The electron temperature, calculated with different wavelengths, as a function of the distance from the launching gap of the surfatron, at 79,6 mbar and a plasma length of 11 cm.



Graph 12: The electron temperature when a different diameter is assumed at 2,3 mbar and 727,3 nm and with a length of 22 cm. The black line is the temperature at the base of the plasma (and known diameter) and thus the reference line. The red line is taken near, but not at, the end of the plasma.